# Fast MBF Based Method for Large Random Array Characterization

David González-Ovejero[1], Eloy de Lera Acedo*[2], Nima Razavi-Ghods[2], and Christophe Craeye[1]

[1] Laboratoire de Télécommunication et Télédétection,
Université catholique de Louvain, 1348 Louvain-la-Neuve, Belgium

E-mail: {david.gonzalez, christophe.craeye}@uclouvain.be

[2] Cavendish Laboratory, University of Cambridge, Cambridge, CB3 0HE, UK

E-mail: {eloy, nima}@mrao.cam.ac.uk

-------------------------------------------------------------------------
*This effort/activity is supported by the European Community Framework Programme 6, Square Kilometre Array Design Studies (SKADS), contract no011938.
-------------------------------------------------------------------------

# Fast MBF Based Method for Large Random Array Characterization

David González-Ovejero[1], Eloy de Lera Acedo*[2], Nima Razavi-Ghods[2], and Christophe Craeye[1]

[1] Laboratoire de Télécommunication et Télédétection,
Université catholique de Louvain, 1348 Louvain-la-Neuve, Belgium
E-mail: {david.gonzalez, christophe.craeye}@uclouvain.be
[2] Cavendish Laboratory, University of Cambridge, Cambridge, CB3 0HE, UK
E-mail: {eloy, nima}@mrao.cam.ac.uk

## Introduction

The new generation of radio telescopes such as the Square Kilometer Array (SKA) [1] relies heavily on the use of very large phased arrays. The current frequency range of the SKA is 0.07-25 GHz and this will be made possible using multiple collector technologies, consisting mainly of dishes at high frequencies (>1GHz) and aperture arrays for the key science of detecting red-shifted hydrogen emission at around 1 GHz and below [1]. In the sub 1 GHz frequency regime, the telescope can provide a million square meters of collecting area, which is two orders of magnitude more sensitivity than current instruments. The lower portion of this band is called AAlo. Operating from 70 to 450 MHz, it will comprise up to hundreds of stations of at least 10000 elements each. Furthermore, the SKA community is considering the use of random sparse configurations instead of the classical regular arrays [2]. The cost in the design process is evident, as now periodic infinite array approaches, available in many commercial simulation packages, are no longer applicable.

The method proposed by the authors to reduce the computational cost devoted to solve the full EM problem in such arrays is based in the Macro Basis Function technique [3, 4] and the interpolation method proposed in [5]. On the other hand, it is shown how the embedded element pattern convergence within a radius of influence allows us to account only for a few tens of significative elements when computing the aforementioned pattern for each antenna. This approximation provides a further computational cost reduction and is a first step towards a very fast full-wave simulation tool for very large random arrays.

## Method of Moments simulation of the Embedded Element Patterns

The proposed Method of Moments (MoM) simulation for this problem relies on the use of Macro Basis Functions (MBFs) [3, 6, 7], also called Characteristic Basis Functions [4, 8], and the interpolation technique presented in [5]. The Macro Basis Functions method consists of reducing the size of the MoM impedance matrix by replacing the original set of elementary basis functions with a new set of functions obtained through the solution of smaller problems. Once the MoM matrix size is reduced by means of the MBF technique, the complexity $\mathcal{O}((N\,A)^3)$ for solving the system of equations is reduced to $\mathcal{O}((Q\,A)^3)$, where $A$ is the number of antennas in the array and $N$ and $Q$ ($Q \ll N$) are the number of elementary and Macro Basis Functions, respectively. Nevertheless, the impedance matrix filling time remains $\mathcal{O}((N\,A)^2)$, and rapidly becomes the dominant operation in the total solution time. To overcome this limitation, the computation of interactions between macro basis functions is carried out by interpolating exact data obtained on a simple grid; thereby

978-1-4244-3647-7/09/$25.00 ©2009 IEEE

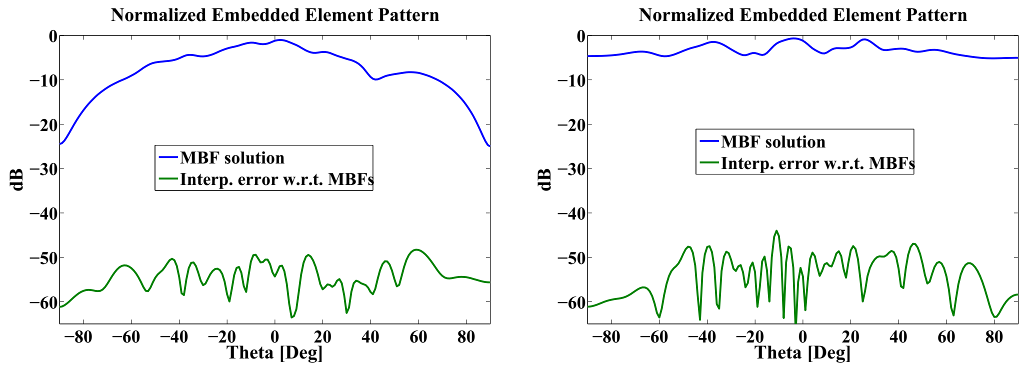


(a) E plane ($\phi = 90^o$)

(b) H plane ($\phi = 0^o$)

Figure 1: Embedded element pattern obtained with the MBF approach and error for the interpolation technique w.r.t MBF solution.

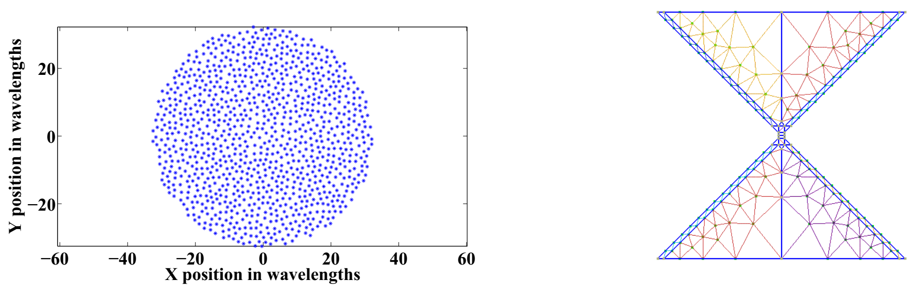


(a) Array layout

(b) Bowtie mesh

Figure 2: Array configuration.

non regular arrays may be easily analyzed as well as optimized. The complexity will be now $\mathcal{O}(P\,N^2 + A^2\,S)$, where $P$ (typically around some tens or very few hundreds) is the number of elements in the grid and $S$ is a very small factor related to the interpolation time. It is interesting to notice that this factor no longer depends on the complexity of the antenna. Therefore a speed up of the order of $A$ can be obtained for sparse arrays.

The performance of the interpolation method is shown in Fig. 1, where the embedded element pattern is computed for one antenna in a random array covering 47 elements. The reduced impedance matrix filling time was 77 minutes when only using MBF and 20 seconds for the interpolation technique (without accounting for the grid generation time) in a standard laptop.

The initial target is to obtain the pattern for an example comprising 1000 bowtie elements, like the one shown in Fig. 2b, randomly placed in a circular area of radius $30\lambda$ (Fig. 2a), which at this point would represent a reduced version of the aforementioned SKA AAlo. For the present analysis the average minimum distance between elements is $1.5\lambda$ and the elements size is $\lambda \times \lambda$. Each port has been loaded with a 200 $\Omega$ series impedance.

In the exact case, the embedded patterns should model, for each antenna in the array, the

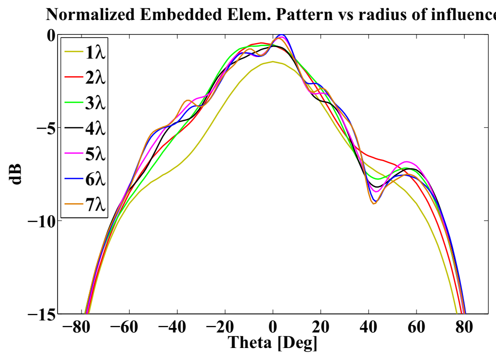


(a) E plane ($\phi = 90^o$)

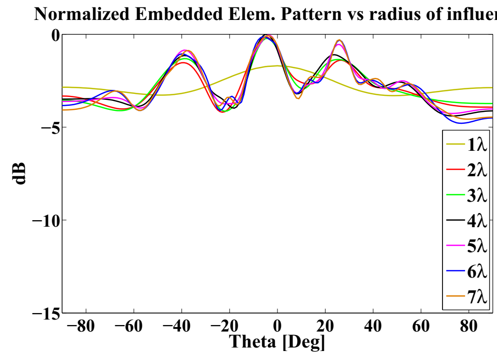


(b) H plane ($\phi = 0^o$)

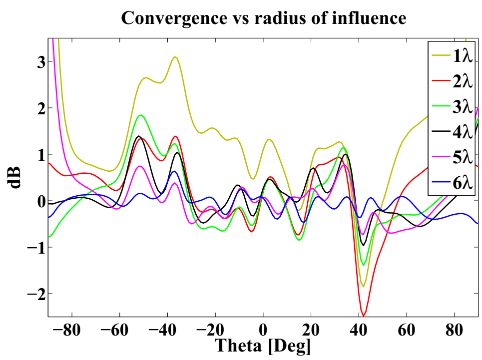


(c) E plane error

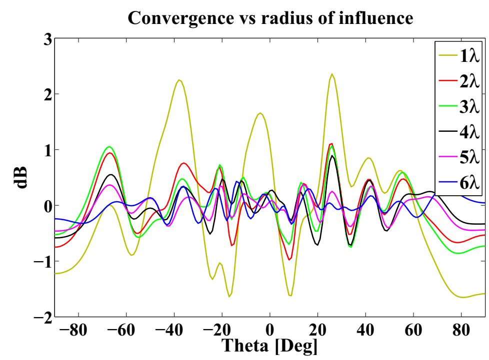


(d) H plane error

Figure 3: Embedded element patterns and errors for different radius of influence.

field radiated by the element of interest excited while the rest of elements in the array are passively terminated. This computation should involve all the elements in the array, though it is not possible within our memory limits (we can simulate up to $\approx 300$ elements with a conventional laptop). Nevertheless, a so-called “radius of influence”, can be defined for every antenna in the array. The embedded pattern is then computed accounting only for the antennas contained in the circle defined by this radius. Assuming that the latter approximation is good enough, the complexity in the calculation of the interactions and the solution of the MoM system of equations by Gaussian elimination can be dramatically reduced.

In order to prove the convergence of the method, Fig. 3a and Fig. 3b show the normalized embedded element pattern in dB for one of the antennas in the array. Both E-plane and H-plane cuts converge reasonably well for a radius of influence larger than $5\lambda$. Fig. 3c and Fig. 3d represent the differential error between the patterns computed for different radii of influence with respect to the pattern calculated for the largest radius considered ($7\lambda$). Again for both planes similarly, the differential error decreases rapidly and seems to converge after $5\lambda$. Once we have the embedded element pattern for each antenna, in order to obtain the total pattern for the proposed array, all the embedded element patterns are combined through the excitation law of interest.

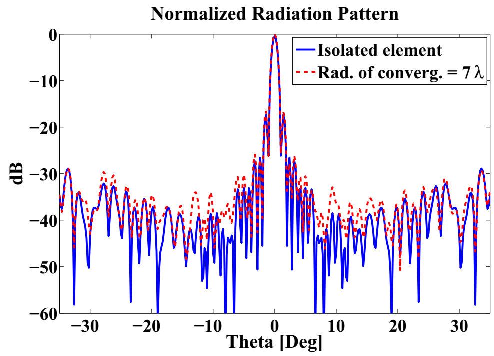

(a) E plane ($\phi = 90^o$)

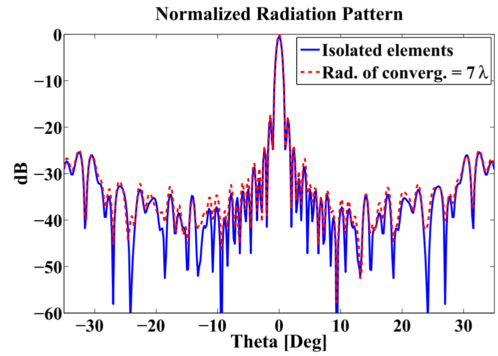

(b) H plane ($\phi = 0^o$)

Figure 4: Array Patterns assuming isolated element patterns and including mutual coupling up to a $7\lambda$ radius.

## Numerical results and conclusion

The array pattern obtained for the example proposed in the previous section is shown in Fig. 4. The result for a $7\lambda$ radius of convergence is compared with the pattern obtained considering only the isolated element pattern, which can also be seen as the embedded element pattern for a radius of influence set to 0. A difference of 0.45 dB is observed at broadside direction between both approaches. It is striking that this difference is much more than what one would expect assuming that the effects of mutual coupling behave like a centered random variable. This bias, as well as more elaborate techniques for the fast array solution will be the focus of further research.

## References


[1] The Square Kilometre Array. [Online]. Available: www.skatelescope.org/

[2] R. Braun and W. van Cappellen. SKA Memo 87: aperture arrays for the SKA: dense or sparse? [Online]. Available: http://www.skatelescope.org/PDF/memos/memo_87.pdf/

[3] E. Suter and J. R. Mosig, "A subdomain multilevel approach for the efficient MoM analysis of large planar antennas," *Microw. Opt. Technol. Lett.*, vol. 26, pp. 270–277, Mar. 2000.

[4] J. Yeo, V. Prakash, and R. Mittra, "Efficient analysis of a class of microstrip antennas using the Characteristic Basis Function Method (CBFM)," *Microw. Opt. Technol. Lett.*, vol. 39, pp. 456–464, Dec. 2003.

[5] D. González-Ovejero and C. Craeye, "Fast computation of Macro Basis Functions interactions in non-uniform arrays," in *Proc. IEEE AP-S Soc. Int. Symp.*, San Diego, CA, Jul. 2008.

[6] C. Craeye, "A fast impedance and pattern computation scheme for finite antenna arrays," *IEEE Trans. Antennas Propag.*, vol. 54, pp. 3030–3034, Oct. 2006.

[7] C. Craeye and R. Sarkis, "Finite array analysis through combination of Macro Basis Functions and Array Scanning Methods," *Journal of Applied Comput. Electromagnetics Soc. (ACES)*, vol. 23, pp. 999–1007, Sep. 2008.

[8] R. Maaskant, R. Mittra, and A. Tijhuis, "Fast analysis of large antenna arrays using the Characteristic Basis Function Method and the Adaptive Cross Approximation Algorithm," *IEEE Trans. Antennas Propag.*, vol. 56, pp. 3440–3451, Nov. 2008.